Deregulation of the tumour suppressor genes $p14^{ARF}$, $p15^{INK4b}$, $p16^{INK4a}$ and p53 in basal cell carcinoma

P. Kanellou, A. Zaravinos, M. Zioga* and D.A. Spandidos

Laboratory of Virology, Medical School, University of Crete, Heraklion 71100, Crete, Greece
**A. Sygros Hospital, Department of Dermatology, Medical School, University of Athens, Athens, Greece*

Summary

Correspondence
D.A. Spandidos.
E-mail: spandidos@spandidos.gr

Accepted for publication
21 December 2008

Key words
basal cell carcinoma, microsatellite instability/loss of heterozygosity, mRNA expression, mutations, $p14^{ARF}$, $p15^{INK4b}$, $p16^{INK4a}$, p53

Conflicts of interest
None declared.

P.K. and A.Z. contributed equally to this work and should be considered as first authors.

DOI 10.1111/j.1365-2133.2009.09079.x

Background Basal cell carcinoma (BCC) is a locally aggressive slowly growing tumour that rarely metastasizes and is mostly seen in older members of the population.

Objectives To determine the involvement of the tumour suppressor genes $p14^{ARF}$, $p15^{INK4b}$, $p16^{INK4a}$ and p53 in BCC.

Methods We investigated the integrity of the *CDKN2A* locus in 15 BCC samples by analysing the presence of allelic imbalance/loss of heterozygosity (LOH). Moreover, we studied the mRNA expression levels of the tumour suppressor genes $p14^{ARF}$, $p15^{INK4b}$, $p16^{INK4a}$ and p53 in the BCC samples and compared them with mRNA levels in the corresponding normal tissue. The presence of mutations was examined by sequencing for exons 1a and 2 of $p16^{INK4a}$.

Results We found LOH in one BCC sample for the marker D9S1748. A polymorphism (G442A) of exon 2 was detected in three cases. $p14^{ARF}$, $p15^{INK4b}$ and p53 presented high expression levels, whereas $p16^{INK4a}$ exhibited low mRNA levels compared with the corresponding normal tissue. Significant correlations were detected among the genes studied.

Conclusions Our results demonstrate a different expression profile between $p16^{INK4a}$ and $p14^{ARF}$, $p15^{INK4b}$ and p53 in BCC. Moreover, we found a low percentage of LOH and of a polymorphic sequence variant (Ala148Thr) for the *CDKN2A* locus.

Basal cell carcinoma (BCC) of the skin is the most common neoplasm among the Caucasian population of the western world.[1–3] Epidemiological data indicate that the overall incidence of BCC is increasing significantly, by about 3–10% annually, worldwide.[4] BCC, a keratinocyte-derived tumour, is a locally aggressive slowly growing tumour that rarely metastasizes[3,5] and is mostly seen in the more elderly members of the population.[6] Many genetic and environmental factors contribute to the development of skin cancer. Of these, solar ultraviolet (UV) radiation—a potent environmental DNA-damaging agent known to induce skin cancer[7–9]—is considered to be the most important. When these mutations affect the function of sufficient numbers of oncogenes, tumour suppressor genes and important housekeeping genes, they result in an uncontrolled cell cycle and the transformation of keratinocytes.[10] As well as causing mutations in DNA directly, UV-altered signal transduction may affect mutation frequency indirectly. For example, it alters the cell cycle, leaving less time for DNA repair prior to the subsequent round of replication, or reduces the levels of the enzymes that protect cells from UV damage.[11] Nevertheless, it can be argued that susceptibility genes also play a potential role in BCC risk, for example based on the observation that these tumours are sometimes found on parts of the body not chronically exposed to the sun.[3,6] The INK4a/ARF (*CDKN2A*) and INK4b (*CDKN2B*) gene loci are located at chromosomal band 9p21. The locus *CDKN2A* encodes two tumour suppressor genes, $p16^{INK4a}$ and $p14^{ARF}$, both involved in the negative control of cell proliferation. They share common exons 2 and 3, but have alternatively spliced first exons (exon 1a for $p16^{INK4a}$ and 1b for $p14^{ARF}$) (Fig. 1). These first exons are under the control of distinct promoters and uniquely create two proteins that have no sequence homology at the amino acid level.[12] $p16^{INK4a}$ is a cyclin-dependent kinase (CDK) 4 inhibitor that specifically acts at the G_1/S phase of the cell cycle by negatively controlling retinoblastoma (Rb) phosphorylation status,[13] while $p14^{ARF}$ binds to Mdm2 (murine double minute), preventing both Mdm2-mediated p53 degradation and Mdm2-mediated Rb inactivation and causing the arrest of the G_1 and G_2 phases of the cell.[14,15] Consequently, stabilized p53 can induce temporary and permanent growth arrest, DNA repair, terminal differentiation or apoptosis in response to oncogenic signals

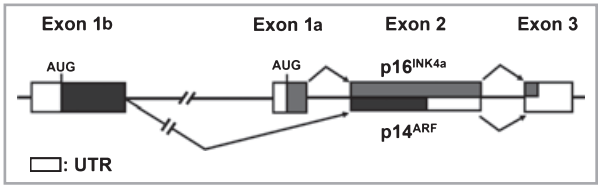

Fig 1. The *CDKN2A* locus structure. UTR, untranslated region.

and DNA damage.[16] $p15^{INK4b}$, another CDK inhibitor gene located in chromosome region 9p21.2, has a strong structural and functional homology to $p16^{INK4a}$,[17] and is transcriptionally activated by transforming growth factor-β.[18] The $p15^{INK4b}$ protein binds to the cdk4–cyclin D complex, displacing p27 and freeing it to bind to and inhibit the cdk2–cyclin E complex required for entry into the S phase of the cell cycle.[19] The $p16^{INK4a}$ and $p14^{ARF}$ genes are found altered in primary tumours such as melanoma and carcinomas of the lung, bladder, breast, oesophagus and head and neck.[17,20–24]

In this study, we investigated the integrity of the *CDKN2A* locus in 15 BCC samples by analysing the presence of allelic imbalance/loss of heterozygosity (LOH) in microsatellite markers. Moreover, we studied the expression levels of the tumour suppressor genes $p14^{ARF}$, $p15^{INK4b}$, $p16^{INK4a}$ and p53 in those BCC samples, and compared them with the corresponding adjacent normal tissue. Furthermore, the presence of mutations was examined by direct sequencing of exons 1a and 2 of $p16^{INK4a}$.

Materials and methods

Tumour specimens and DNA extraction

Fifteen BCC/normal tissue paired samples were obtained from patients treated at 'A. Sygros' Hospital (Athens, Greece) with the approval of the donors and the Institute's ethical committee. All samples were histopathologically examined by an experienced pathologist prior to DNA extraction. Extreme effort was made to avoid any adjacent normal tissue and to isolate areas of tissue containing > 70% tumour cells. Clinicopathological characteristics of the patients are depicted in Table 1. Immediately following dissection, the specimens were stored at −80 °C until DNA extraction. A matched DNA control from blood was analysed. Genomic DNA was extracted using proteinase K, followed by phenol/chloroform extraction and ethanol precipitation. All specimens were examined for the presence of amplifiable DNA using a set of primers for the β-globin gene.

Microsatellite instability/loss of heterozygosity analysis

The DNA sample and matched blood or genomic DNA of each patient were analysed for genetic alterations using five highly polymorphic microsatellite (dinucleotide repeat) markers. The selection of the chromosome region examined and of the markers used was based on previous studies on skin cancer that have shown chromosomal locations exhibiting a variable degree of alteration. Three markers, D9S171, D9S1748 and D9S974, were chosen because of their location with respect to the *CDKN2A* exons (chromosome 9p21). In addition, all have a high informativity rate (heterozygosity score) and produce a polymerase chain reaction (PCR) product small enough for the successful amplification of DNA. The markers D17250 and *TP53* were used to detect LOH in the regions 17q21 and 17p13.1, respectively. All primer oligonucleotide sequences and amplification conditions used were as before,[25] and genotyping was performed on a LICOR Long ReadIR^2 4200 DNA sequencer (Li-Cor Biosciences, Lincoln, NE, U.S.A.) as previously reported. Analysis was performed at least twice and the results were highly reproducible.

Table 1 Clinicopathological characteristics of the patients (n = 15)

M/F	10/5
Age (years)	65–82
Mean ± SD	75 ± 7·5
Site of BCC lesion, n	
Forehead/temples	10
Cheek	2
Nose	1
Hand	1
Leg	1
Medical history, n	
Skin cancer	7
Other type of cancer/immunosuppression	0

BCC, basal cell carcinoma.

Mutational analysis

Exon 2 of both the $p16^{INK4a}$ and $p14^{ARF}$ genes and the alternatively spliced exon 1a of $p16^{INK4a}$ were amplified by PCR from genomic DNA with the use of primers complementary to their flanking intron sequences. The sequences of the primers for exon 2 and exon 1a have previously been identified.[26] PCR was carried out under standard conditions as described above. Dimethyl sulphoxide (5%) was added to the reaction buffers for both nucleotide sequencing and PCR amplification. The reactions were denatured for 3 min at 94 °C, and the DNA was subsequently amplified for 40 cycles at 94 °C, 60 °C (for exon 1b), 61 °C (for exon 2) and 72 °C at each step, followed by a final extension step at 72 °C for 10 min. The PCR products were resolved through 2% agarose gel, excised and purified (QIAquick Gel Extraction Kit; Qiagen, Hilden, Germany) to remove unincorporated primers and dNTPs. The sequencing reaction contained 4 μL Big Dye Terminator ready-reaction mix (PE ABI, Warrington, U.K.), 2 μL of the purified PCR product and 1·6 pmol of sequencing primer in a total reaction volume of 10 μL. Reaction conditions were: 96 °C for 10 s, 50 °C for 10 s and 60 °C for 4 min, for 25 cycles. Sequencing products were precipitated with isopropanol to remove

unincorporated dye terminators and resuspended in 10 μL of loading buffer (formamide : dextran sulphate/ethylenediamine tetraacetic acid, 5 : 1). Products were run on a 377 ABI PRISM automatic sequencer and analysed with Sequencing Analysis software (PE ABI).

RNA extraction and reverse transcription

Tissue specimens were homogenized in TRIzol® reagent (Invitrogen, Carlsbad, CA, U.S.A.) using a power homogenizer, followed by chloroform addition and centrifugation. Total RNA was precipitated from the supernatant with isopropanol, washed with 75% ethanol and resuspended in 50 μL diethylpyrocarbonate-treated water. The concentration and purity of the RNA were calculated based, respectively, on the measurement of its 260-nm and 260/280-nm absorbance ratios using a UV spectrophotometer. cDNA was synthesized by reverse transcription with a TaqMan® Reverse Transcription reagents kit (Applied Biosystems, Foster City, CA, U.S.A.). In detail, reverse transcription buffer (10 ×), 2 μg of total RNA, 2·5 μmol L^{-1} of random hexamers, 500 μL dNTPs, 0·4 U μL^{-1} RNase inhibitor, 1·25 U μL^{-1} MultiScribe Reverse Transcriptase and RNase-free water, to a total volume of 20 μL, were incubated at 25 °C for 10 min and heated at 48 °C for 30 min followed by enzyme inactivation at 95 °C for 5 min.

Real-time polymerase chain reaction

CDKN2A, *CDKN2B* and p53 mRNA expression was measured using a real-time PCR assay with SYBR®-Green I. All primer pairs were designed to span at least one intron in order to avoid the amplification of contaminating genomic DNA along with the cDNA (Fig. 2). Primer pairs and amplification conditions used were as previously reported[25] with the Mx3000P real-time PCR thermal cycler (Stratagene, La Jolla, CA, U.S.A.). Glyceraldehyde-3-phosphate dehydrogenase (*GAPDH*) was used as an internal control to normalize *CDKN2A*, *CDKN2B* and p53 expression levels. Specifically, 1 μL cDNA from the BCC samples was amplified in a PCR reaction containing 2 × Brilliant SYBR-Green I QPCR Master Mix, 300 nmol L^{-1} of each primer and 30 μmol L^{-1} ROX® passive reference dye in a final volume of 20 μL.

In order to verify the results of the melt curve analysis, PCR products were analysed by electrophoresis on 2% agarose gel, stained with ethidium bromide and photographed on a UV transilluminator. Two nontemplate controls were included in each PCR reaction.

All reactions were run in triplicate, and the *CDKN2A*, *CDKN2B* and p53 transcript levels were calculated and normalized to each specimen's housekeeping gene mRNA (*GAPDH*) as well as to the appropriate calibrators. Relative quantification was performed using the ΔΔCt method, as previously described.[27] A 2-fold increased (≥ 2) or decreased (≤ 0·5) value was considered mRNA overexpression or downregulation, respectively, in that skin sample.

Statistical analysis

The nonparametric Spearman rank correlation was used to examine the pair-wise relation of the genes' mRNA levels and their association with continuous variables (age, sex, sun exposure, site of lesion, duration of lesion, history of sun burns, prior skin cancer and concomitant tumour). The Mann–Whitney U and Kruskal–Wallis H tests were used, when indicated by the analysis, to examine *CDKN2* loci expression status with various clinicopathological parameters after stratification. All statistical analyses were performed with SPSS 11.5 (SPSS, Chicago, IL, U.S.A.). Statistical significance was set at the 95% level ($P < 0·05$).

Results

Loss of heterozygosity/microsatellite instability analysis

Only one BCC sample displayed LOH for the marker D9S1748, whereas no instability was noted for any of the samples in the aforementioned markers (Fig. 3a).

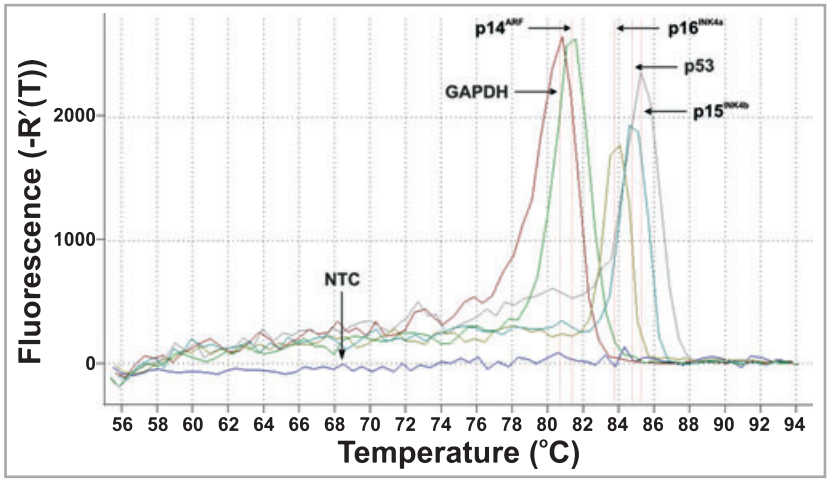

Fig 2. Melt curve analysis for the $p14^{ARF}$, $p15^{INK4b}$, $p16^{INK4a}$, p53 and glyceraldehyde-3-phosphate dehydrogenase (*GAPDH*) genes. Single peaks for all genes and the absence of peaks for the nontemplate controls (NTCs) demonstrates the exclusion of any genomic DNA contamination and the specificity of the polymerase chain reaction products.

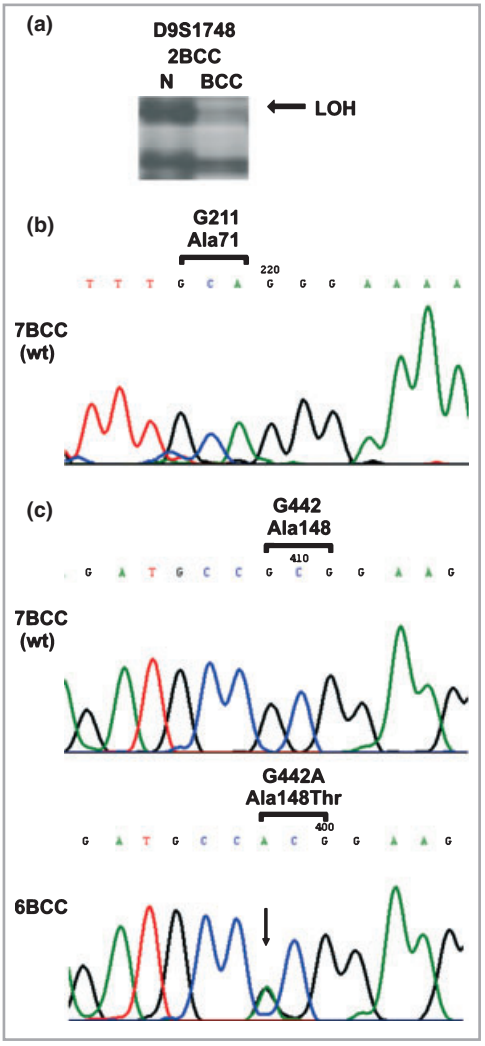

Fig 3. (a) One loss of heterozygosity (LOH) for the marker D9S1748 was detected in the 15 basal cell carcinoma (BCC) samples. The arrow indicates the position of the deleted allele. The faint band in the position of the deleted allele is interpreted as contamination by adjacent normal DNA (N). (b) Representative electropherogram presenting the wild-type (wt) sequence in exon 1a of the *CDKN2A* gene at nucleotide 213. (c) Comparative presentation of sequencing electropherograms in exon 2 of the p16^{INK4a} gene. The upper panel depicts the wt sequence, while the lower panel shows a sample heterozygous for the G > A polymorphism at base 442 (Ala148Thr). The relevant area is marked with an arrow.

CDKN2A polymorphisms – analysis of the p16^{INK4a} gene

We screened 15 BCC cases for germline mutations. Exon 2, common to both genes, and the alternatively spliced exon 1a of p16^{INK4a} were amplified by PCR from genomic DNA with the use of primers complementary to their flanking intron sequences. We found a previously described polymorphic sequence variant[25,26,28] of the *CDKN2A* gene, a G > A transition at base 442 of exon 2 that results in an alanine to threonine substitution at codon 148 (Ala148Thr) (Fig. 3c). This was detected in three of the 15 cases (20%). The Ala148Thr polymorphism does not have to influence the regular function of p16^{INK4a}, as it was demonstrated that it has the same potency to inhibit cyclin D1/CDK4 and cyclin D1/CDK6 as the wild-type protein. Additionally, there was no sequence variant detected in any of the patients concerning the unique exon 1a of the p16^{INK4a} gene (Fig. 3b).

Characterization of the p14^{ARF}, p15^{INK4b}, p16^{INK4a} and p53 gene expression levels

Table 2 depicts the expression levels of the genes studied in the BCC tissues. All the tumour suppressor genes were expressed in all the samples. The genes p14^{ARF}, p15^{INK4b} and p53 presented a similar expression pattern, exhibiting underexpression in around 13–20% of the samples, whereas a significant percentage (40–67%) exhibited high transcript levels. However, in 11 BCC samples p16^{INK4a} exhibited low levels of expression compared with the corresponding normal tissue (mean fold ± SD was 0·27 ± 0·15) and three samples (20%) showed equal levels of expression between the two tissue types (0·85-fold), while only one sample exhibited 14-fold overexpression compared with the corresponding control tissue. No statistical significance in the mRNA levels of the tumour suppressor genes studied could be discerned between the pathological tissue and the corresponding phenotypically normal tissue (Fig. 4).

mRNA expression pair-wise analysis and correlation between loss of heterozygosity/microsatellite instability analysis results and expression of the tumour suppressor genes

The Spearman test was run in order to detect possible correlations in the evaluation of the coexpression patterns of the tumour suppressor genes in the BCC and normal skin tissue groups. The results are displayed in Table 3. Specifically, in BCC a positive correlation between p14^{ARF} and p15^{INK4b}

Table 2 Expression status of the tumour suppressor genes studied in basal cell carcinoma compared with the adjacent normal tissue (n = 15)

	Relative mRNA expression		
Gene	↑ (%), mean ± SD	— (%), mean ± SD	↓ (%), mean ± SD
p14^{ARF}	10/15 (67)	3/15 (20)	2/15 (13)
	3·03 ± 1·35	1·43 ± 0·50	0·29 ± 0·08
p15^{INK4b}	7/15 (47)	5/15 (33)	3/15 (20)
	3·09 ± 1·36	1·67 ± 0·25	0·21 ± 0·21
p16^{INK4a}	1/15 (7)	3/15 (20)	11/15 (73)
	14·03 ± 0·0	0·85 ± 0·33	0·27 ± 0·15
p53	6/15 (40)	7/15 (47)	2/15 (13)
	2·99 ± 1·54	1·39 ± 0·46	0·12 ± 0·14

↑, overexpression; —, equally expressed samples; ↓, underexpression.

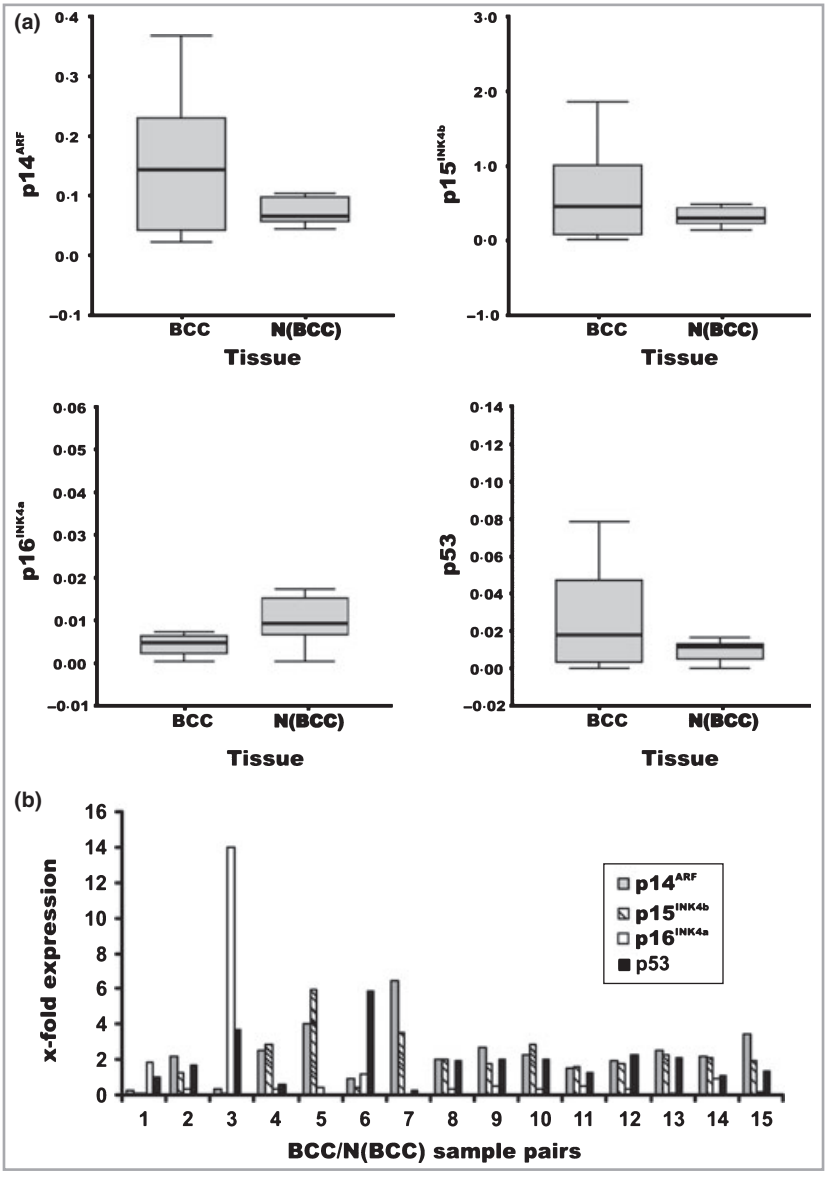

Fig 4. (a) mRNA levels of the $p14^{ARF}$, $p15^{INK4b}$, $p16^{INK4a}$ and p53 genes. The majority of the $p14^{ARF}$, $p15^{INK4b}$ and p53 genes exhibited higher expression levels in the basal cell carcinoma (BCC) than in the normal tissue adjacent to the BCC sample [N(BCC)]. However, $p16^{INK4a}$ presented the reverse expression pattern, being underexpressed in the majority of BCC samples. No statistically significant difference could be deduced. Box plots show the 25th, 50th (median) and 75th percentile values. Whiskers show the minimum and maximum values. (b) Summary of the mRNA expression levels of the $p14^{ARF}$, $p15^{INK4b}$, $p16^{INK4a}$ and p53 genes in BCC compared with N(BCC).

($P = 0{\cdot}002$) and a negative correlation between p53 and $p15^{INK4b}$ ($P = 0{\cdot}020$) was found. Conversely, these correlations were absent in the normal skin tissue, and the negative correlation between $p15^{INK4b}$ and $p16^{INK4a}$ found in the normal tissue ($P < 0{\cdot}001$) was lost in the BCC samples. Moreover, a negative correlation between p53 and $p14^{ARF}$ was present in both BCC and its adjacent normal tissue ($P = 0{\cdot}014$ and $P = 0{\cdot}011$, respectively).

The only BCC sample that displayed LOH at the D9S1748 marker exhibited underexpression of $p16^{INK4a}$ and overexpression of $p14^{ARF}$.

Discussion

We found a low incidence of LOH confined to chromosome arm 9p in one of the 15 BCC samples examined for the microsatellite marker D9S1748. Our data confirm the results of two previous studies reported by Quinn *et al.*[5,29] However, they are contrary to other studies reporting a significantly higher incidence of LOH on the 9p arm,[2,3,30] perhaps due to differences in the markers used and in the number of specimens examined.

We did not screen the $p15^{INK4b}$ gene because, to date, no mutations of this gene have been reported in melanoma kindreds.[31]

As previously reported by Saridaki *et al.*,[3] we found the G442A (Ala148Thr) polymorphic sequence variant in the *CDKN2A* gene in three of 15 BCC samples. However, all the BCCs were characterized by the lack of mutations in exon 1a of $p16^{INK4a}$, in contrast to our last report regarding squamous cell carcinoma (SCC), where novel mutations were detected on this exon.[25]

We noted a 40% rate of p53 overexpression in BCC compared with the adjacent normal tissue, while more than half of the BCC samples (67%) exhibited increased levels of $p14^{ARF}$, noted also by the negative correlation between the

Table 3 $p14^{ARF}$, $p15^{INK4b}$, $p16^{INK4a}$ and p53 pair-wise coexpression analysis in basal cell carcinoma (BCC) and normal skin tissue [N(BCC)]

		$p14^{ARF}$	$p15^{INK4b}$	$p16^{INK4a}$	p53
BCC					
$p14^{ARF}$	CC	1·000	–	–	–
	P-value	–	–	–	–
$p15^{INK4b}$	CC	0·851[b]	1·000	–	–
	P-value	**0·002**	–	–	–
$p16^{INK4a}$	CC	−0·317	−0·203	1·000	–
	P-value	0·373	0·575	–	–
p53	CC	−0·801[a]	−0·714[a]	0·709[a]	1·000
	P-value	**0·014**	**< 0·020**	**0·022**	–
N(BCC)					
$p14^{ARF}$	CC	1·000	–	–	–
	P-value	–	–	–	–
$p15^{INK4b}$	CC	0·087	1·000	–	–
	P-value	0·853	–	–	–
$p16^{INK4a}$	CC	−0·087	−1·000[b]	1·000	–
	P-value	0·853	**< 0·001**	–	–
p53	CC	−0·871[a]	0·087	0·090	1·000
	P-value	**0·011**	0·080	0·862	–

[a]Correlation is significant at the 0·05 level (two-tailed); [b]correlation is significant at the 0·01 level (two-tailed). CC, correlation coefficient. Significant correlations are shown in bold.

two genes. A possible explanation for this observation is the role played by p53 in protecting cells from DNA damage, which results in these transformed keratinocytes undergoing apoptosis.[32] Loss of $p14^{ARF}$ has been suggested to be functionally equivalent to p53 inactivation as $p14^{ARF}$ stabilizes p53; therefore, cells lacking p53 are resistant to $p14^{ARF}$-induced arrest.[33,34]

In the presence of both $p16^{INK4a}$ and $p15^{INK4b}$, $p16^{INK4a}$ forms more stable binary complexes with both CDK4 and CDK6, thus displacing and leading to the degradation of $p15^{INK4b}$. However, upon the loss of $p16^{INK4a}$, CDK4 inhibition is maintained by $p15^{INK4b}$. This could possibly explain the high percentage (47%) of $p15^{INK4b}$ overexpression observed, while the majority of the samples (73%) exhibited $p16^{INK4a}$ underexpression, as expected. Therefore, the inactivation of the $p16^{INK4a}$ gene product might be the result of reduced expression levels, apart from LOH, promoter hypermethylation and/or mutations in the INK4a/ARF locus.[35]

However, despite the fact that this inactivation is commonly associated with more malignant features in many tumours,[36] including BCC,[37–42] there are recent reports stating a strong $p16^{INK4a}$ mRNA expression in BCC skin.[43–45] Eshkoor *et al.*[43] recently found a significant protein and mRNA expression in BCC cells when compared with normal skin tissue. However, the samples they tested were paraffin-embedded skin BCC, and not freshly frozen tissue. Moreover, apart from phylogenetic differences (Iranian tissue samples), conflicting results could be attributed to different methods used, which demands a strict determination of optimum experimental conditions. Furthermore, there appears to be a strong relationship between the level of invasiveness and expression of $p16^{INK4a}$. The results of Svensson *et al.*[44] linked $p16^{INK4a}$ expression to a highly invasive BCC subtype with infiltrative growth patterns, followed by ceased proliferation. However, the results of Conscience *et al.*[45] appear to conflict with those of Svensson *et al.*, as they did not observe any difference in the expression of $p16^{INK4a}$ among different histological types of carcinoma (BCC, SCC and Bowen's disease), and suggested that $p16^{INK4a}$ expression does not correlate with the degree of proliferation and malignancy. Instead Conscience *et al.* stated that $p16^{INK4a}$ overexpression is significantly associated with the location on sun-exposed areas.

In conclusion, our results demonstrate a different expression profile between $p16^{INK4a}$ and $p14^{ARF}$, $p15^{INK4b}$ and p53 in BCC. Our data emphasize the importance of a group of tumour suppressor genes in BCC, especially that of $p16^{INK4a}$, which appears to be inactivated by low transcript levels, apart from LOH, promoter hypermethylation, and/or mutations in the *CDKN2A* locus. Moreover, we found a low percentage of LOH and of a polymorphic sequence variant (Ala148Thr) for the *CDKN2A* locus. However, the subsequent mechanisms of carcinogenesis still remain unclear.

References

1 Miller DL, Weinstock MA. Nonmelanoma skin cancer in the United States: incidence. *J Am Acad Dermatol* 1994; **30**:774–8.
2 Gailani MR, Leffell DJ, Ziegler A *et al.* Relationship between sunlight exposure and a key genetic alteration in basal cell carcinoma. *J Natl Cancer Inst* 1996; **88**:349–54.
3 Saridaki Z, Koumantaki E, Liloglou T *et al.* High frequency of loss of heterozygosity on chromosome region 9p21-p22 but lack of p16INK4a/p19ARF mutations in Greek patients with basal cell carcinoma of the skin. *J Invest Dermatol* 2000; **115**:719–25.
4 Roewert-Huber J, Lange-Asschenfeldt B, Stockfleth E *et al.* Epidemiology and aetiology of basal cell carcinoma. *Br J Dermatol* 2007; **157** (Suppl. 2):47–51.
5 Quinn AG, Campbell C, Healy E *et al.* Chromosome 9 allele loss occurs in both basal and squamous cell carcinomas of the skin. *J Invest Dermatol* 1994; **102**:300–3.
6 D'Errico M, Calcagnile AS, Corona R *et al.* p53 mutations and chromosome instability in basal cell carcinomas developed at an early or late age. *Cancer Res* 1997; **57**:747–52.
7 Oro AE, Higgins KM, Hu Z *et al.* Basal cell carcinomas in mice overexpressing sonic hedgehog. *Science* 1997; **276**:817–21.
8 Aszterbaum M, Beech J, Epstein EH Jr. Ultraviolet radiation mutagenesis of hedgehog pathway genes in basal cell carcinomas. *J Investig Dermatol Symp Proc* 1999; **4**:41–5.
9 Aszterbaum M, Epstein J, Oro A *et al.* Ultraviolet and ionizing radiation enhance the growth of BCCs and trichoblastomas in patched heterozygous knockout mice. *Nat Med* 1999; **5**:1285–91.
10 Kramer M, Stein B, Mai S *et al.* Radiation-induced activation of transcription factors in mammalian cells. *Radiat Environ Biophys* 1990; **29**:303–13.
11 Daya-Grosjean L, Dumaz N, Sarasin A. The specificity of p53 mutation spectra in sunlight induced human cancers. *J Photochem Photobiol B* 1995; **28**:115–24.
12 Stone S, Dayananth P, Jiang P *et al.* Genomic structure, expression and mutational analysis of the P15 (MTS2) gene. *Oncogene* 1995; **11**:987–91.

13 Serrano M, Hannon GJ, Beach D. A new regulatory motif in cell-cycle control causing specific inhibition of cyclin D/CDK4. *Nature* 1993; **366**:704–7.
14 Bates S, Phillips AC, Clark PA *et al.* p14ARF links the tumour suppressors RB and p53. *Nature* 1998; **395**:124–5.
15 Stott FJ, Bates S, James MC *et al.* The alternative product from the human *CDKN2A* locus, p14(ARF), participates in a regulatory feedback loop with p53 and MDM2. *EMBO J* 1998; **17**:5001–14.
16 Levine AJ. p53, the cellular gatekeeper for growth and division. *Cell* 1997; **88**:323–31.
17 Kamb A, Gruis NA, Weaver-Feldhaus J *et al.* A cell cycle regulator potentially involved in genesis of many tumor types. *Science* 1994; **264**:436–40.
18 Hannon GJ, Beach D. p15INK4B is a potential effector of TGF-beta-induced cell cycle arrest. *Nature* 1994; **371**:257–61.
19 Sherr CJ. The INK4a/ARF network in tumour suppression. *Nat Rev Mol Cell Biol* 2001; **2**:731–7.
20 Wagner SN, Wagner C, Briedigkeit L *et al.* Homozygous deletion of the p16INK4a and the p15INK4b tumour suppressor genes in a subset of human sporadic cutaneous malignant melanoma. *Br J Dermatol* 1998; **138**:13–21.
21 Reed JA, Loganzo F Jr, Shea CR *et al.* Loss of expression of the p16/cyclin-dependent kinase inhibitor 2 tumor suppressor gene in melanocytic lesions correlates with invasive stage of tumor progression. *Cancer Res* 1995; **55**:2713–18.
22 Healy E, Rehman I, Angus B *et al.* Loss of heterozygosity in sporadic primary cutaneous melanoma. *Genes Chromosomes Cancer* 1995; **12**:152–6.
23 Healy E, Belgaid CE, Takata M *et al.* Allelotypes of primary cutaneous melanoma and benign melanocytic nevi. *Cancer Res* 1996; **56**:589–93.
24 Healy E, Belgaid C, Takata M *et al.* Prognostic significance of allelic losses in primary melanoma. *Oncogene* 1998; **16**:2213–18.
25 Kanellou P, Zaravinos A, Zioga M *et al.* Genomic instability, mutations and expression analysis of the tumour suppressor genes p14(ARF), p15(INK4b), p16(INK4a) and p53 in actinic keratosis. *Cancer Lett* 2008; **264**:145–61.
26 Fargnoli MC, Chimenti S, Keller G *et al.* *CDKN2a*/p16INK4a mutations and lack of p19ARF involvement in familial melanoma kindreds. *J Invest Dermatol* 1998; **111**:1202–6.
27 Zaravinos A, Bizakis J, Soufla G *et al.* Mutations and differential expression of the ras family genes in human nasal polyposis. *Int J Oncol* 2007; **31**:1051–9.
28 Jiang P, Stone S, Wagner R *et al.* Comparative analysis of *Homo sapiens* and *Mus musculus* cyclin-dependent kinase (CDK) inhibitor genes p16 (MTS1) and p15 (MTS2). *J Mol Evol* 1995; **41**:795–802.
29 Quinn AG, Sikkink S, Rees JL. Delineation of two distinct deleted regions on chromosome 9 in human non-melanoma skin cancers. *Genes Chromosomes Cancer* 1994; **11**:222–5.
30 Gailani MR, Bale SJ, Leffell DJ *et al.* Developmental defects in Gorlin syndrome related to a putative tumor suppressor gene on chromosome 9. *Cell* 1992; **69**:111–17.
31 Flores JF, Pollock PM, Walker GJ *et al.* Analysis of the *CDKN2A*, *CDKN2B* and *CDK4* genes in 48 Australian melanoma kindreds. *Oncogene* 1997; **15**:2999–3005.
32 Hussein MR, Sun M, Tuthill RJ *et al.* Comprehensive analysis of 112 melanocytic skin lesions demonstrates microsatellite instability in melanomas and dysplastic nevi, but not in benign nevi. *J Cutan Pathol* 2001; **28**:343–50.
33 Saridaki Z, Liloglou T, Zafiropoulos A *et al.* Mutational analysis of *CDKN2A* genes in patients with squamous cell carcinoma of the skin. *Br J Dermatol* 2003; **148**:638–48.
34 Ribeiro GR, Francisco G, Teixeira LV *et al.* Repetitive DNA alterations in human skin cancers. *J Dermatol Sci* 2004; **36**:79–86.
35 Hanahan D, Weinberg RA. The hallmarks of cancer. *Cell* 2000; **100**:57–70.
36 Sherr CJ. Cancer cell cycles. *Science* 1996; **274**:1672–7.
37 Bianchi AB, Fischer SM, Robles AI *et al.* Overexpression of cyclin D1 in mouse skin carcinogenesis. *Oncogene* 1993; **8**:1127–33.
38 Yamamoto H, Ochiya T, Takeshita F *et al.* Enhanced skin carcinogenesis in cyclin D1-conditional transgenic mice: cyclin D1 alters keratinocyte response to calcium-induced terminal differentiation. *Cancer Res* 2002; **62**:1641–7.
39 Sauter ER, Nesbit M, Litwin S *et al.* Antisense cyclin D1 induces apoptosis and tumor shrinkage in human squamous carcinomas. *Cancer Res* 1999; **59**:4876–81.
40 Nindl I, Meyer T, Schmook T *et al.* Human papillomavirus and overexpression of P16INK4a in nonmelanoma skin cancer. *Dermatol Surg* 2004; **30**:409–14.
41 Nakamura S, Nishioka K. Enhanced expression of p16 in seborrhoeic keratosis; a lesion of accumulated senescent epidermal cells in G1 arrest. *Br J Dermatol* 2003; **149**:560–5.
42 Nilsson K, Svensson S, Landberg G. Retinoblastoma protein function and p16INK4a expression in actinic keratosis, squamous cell carcinoma *in situ* and invasive squamous cell carcinoma of the skin and links between p16INK4a expression and infiltrative behavior. *Mod Pathol* 2004; **17**:1464–74.
43 Eshkoor SA, Ismail P, Rahman SA *et al.* p16 gene expression in basal cell carcinoma. *Arch Med Res* 2008; **39**:668–73.
44 Svensson S, Nilsson K, Ringberg A *et al.* Invade or proliferate? Two contrasting events in malignant behavior governed by p16(INK4a) and an intact Rb pathway illustrated by a model system of basal cell carcinoma. *Cancer Res* 2003; **63**:1737–42.
45 Conscience I, Jovenin N, Coissard C *et al.* P16 is overexpressed in cutaneous carcinomas located on sun-exposed areas. *Eur J Dermatol* 2006; **16**:518–22.

